Short-Range Test of the Equivalence Principle

J. H. Gundlach, G. L. Smith, E. G. Adelberger, B. R. Heckel, and H. E. Swanson
Department of Physics, University of Washington, Seattle, Washington 98195
(Received 26 November 1996)

We rotated a 3 ton ^{238}U attractor around a compact torsion balance and compared the accelerations of Cu and Pb toward U. We found that $a_{\mathrm{Cu}} - a_{\mathrm{Pb}} = (-0.7 \pm 5.7) \times 10^{-13}$ cm/s^2, compared to the 9.8×10^{-5} cm/s^2 gravitational acceleration toward the attractor. Our results set new constraints on equivalence-principle violating interactions with Yukawa ranges down to 1 cm and rule out an earlier suggestion of a Yukawa interaction coupled predominantly to $N - Z$. [S0031-9007(97)02847-0]

PACS numbers: 04.80.Cc

The equivalence principle, the notion that gravitation is equivalent to an acceleration of the reference frame, may be tested by comparing the accelerations of test bodies toward a massive attractor. For maximum sensitivity, the test bodies should have relevant properties (binding energy per unit mass, atomic charge Z, neutron-to-proton ratio N/Z, etc.) that differ by the greatest practical amount. The classic equivalence-principle tests [1,2] compared the accelerations of test bodies toward the sun, implicitly assuming that any violation of the equivalence principle (more precisely, of the universality of free fall or UFF) would have an infinite range. This paper presents the latest result in our program to test the UFF with as much generality as is practical.

For such tests, we imagine that a UFF-violating interaction between point bodies has a Yukawa form

$$V_{12}(r) = \mp \frac{g^2}{4\pi} q_1 q_2 \frac{e^{-r/\lambda}}{r}, \qquad (1)$$

where g is a coupling constant, q is the "charge" of a body (not to be confused with electrical charge), λ is the interaction range, and the $-$ and $+$ signs correspond to interactions mediated by scalar or vector bosons, respectively. We make no *a priori* assumptions concerning q, λ, or the scalar or vector nature of the interaction. The interaction in Eq. (1) would lead to a differential acceleration of test bodies 1 and 2 toward an attractor A

$$\frac{\Delta \vec{a}}{a_g} = \alpha \left[\left(\frac{q}{\mu}\right)_1 - \left(\frac{q}{\mu}\right)_2 \right] \left(\frac{q}{\mu}\right)_A \vec{I}(\lambda), \qquad (2)$$

where a_g is the gravitational acceleration toward A, $\alpha = \mp g^2/(4\pi G u^2)$ is dimensionless, u is the atomic mass unit, μ refers to the mass in u, and $\vec{I}(\lambda)$ involves an integral over the attractor and pendulum density distributions.

We recently reported tests of the UFF for Be, Al, Si/Al, and Cu test bodies attracted toward Earth, Sun, and our galaxy [3]. This paper describes a comparison of the accelerations of Cu and Pb toward a 3 ton uranium attractor. We undertook this new work for the following reasons. Our torsion-balance test using Earth and its local topography as the attractor had good sensitivity to UFF-violating interactions with 1 m $\leq \lambda \leq \infty$ except for a gap between $\lambda = 10$ km and $\lambda = 1000$ km. The lower limit on λ was set by the distance from our instrument to the nearest substantial mass, while the gap occurred because at these ranges we could not reliably compute $\vec{I}(\lambda)$ to find the horizontal Yukawa acceleration to which torsion-balances are sensitive. Furthermore, all Earth-attractor results have little sensitivity to UFF-violating interactions with $q \propto N - Z$ because the earth contains nearly equal numbers of neutrons and protons. Our new test uses a ^{238}U attractor because its density $\rho \approx 18.2$ g/cm^3 [4] is very high, its neutron excess, $(N - Z)/(N + Z) = 0.23$, differs substantially from the terrestrial excess of ≈ 0, and we can compute $\vec{I}(\lambda)$ for any λ [5]. The high density allowed us to design an instrument with very close geometry and good sensitivity to interactions with λ's down to 1 cm, corresponding to exchanged bosons with masses up to 2×10^{-5} eV. In addition, the attractor was large enough that we could improve on previous constraints in the "gap region" derived from Galileo-type comparisons of vertical accelerations [6,7].

Our Rot-Wash instrument is shown in Fig. 1. A specially shaped 2620 kg depleted uranium attractor revolved slowly and uniformly around a stationary torsion balance containing 2 Cu and 2 Pb test bodies configured as a composition dipole. A UFF-violating interaction would apply a torque to the pendulum that varied as the sine of the azimuthal angle, ϕ, between the uranium attractor and composition dipole

$$T = \alpha\, s\, M\, a_g \left[\left(\frac{q}{\mu}\right)_{\mathrm{Cu}} - \left(\frac{q}{\mu}\right)_{\mathrm{Pb}} \right] \left[\frac{q}{\mu} \right]_A I(\lambda) \sin\phi\,, \qquad (3)$$

where $M = 9.974$ g is a test-body mass, and $s = 4.31$ cm the distance between centers of adjacent test bodies. Because of the close geometry we devoted much effort to avoiding spurious signals from gravity gradients. Gravity-gradient torques are proportional to the products of the spherical multipole moments, q_{lm}, of the pendulum and the multipole fields of the attractor Q_{lm},

$$T_g = -4\pi G \sum_{l=2}^{\infty} \frac{1}{2l+1} \sum_{m=-l}^{l} q_{lm} Q_{lm} m e^{-im\phi}, \qquad (4)$$

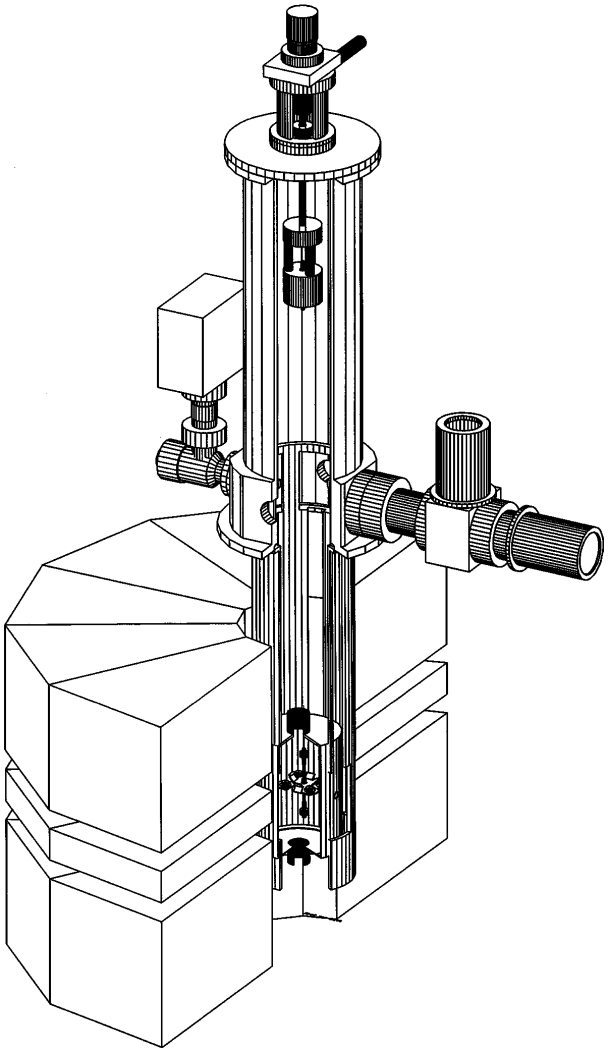

FIG. 1. Schematic view of the Rot-Wash instrument. The 2620 kg ^{238}U attractor had inner and outer radii of 10.2 and 44.6 cm, respectively. The ^{238}U was counterbalanced by 820 kg of Pb so the floor would not tilt as the attractor revolved. Small Pb blocks that reduced the attractor's stray Q_{21} and Q_{31} fields are not shown. The turntable is omitted for clarity. The torsion balance was surrounded by a constant-temperature enclosure and the entire apparatus resided inside a temperature-controlled shed.

where our notation is defined in Refs. [3,5]; the sum begins with $l = 2$ because the $l = 1$ moments vanish for a pendulum suspended from a perfectly flexible fiber. The $m = 1$ torques are particularly troublesome because they have the same frequency as the UFF-violating signal.

The attractor spanned 180°of azimuth and was divided into three segments by two horizontal gaps designed to eliminate the Q_{31} and Q_{51} fields. The $Q_{21}, Q_{41}, Q_{61}, \ldots$, fields nominally vanish by symmetry. The three attractor segments were separated by nonmagnetic bearings so we could rotate the upper two segments with respect to the lowest segment to produce large Q_{21} or Q_{31} fields for measuring gravity-gradient effects as discussed below.

The pendulum, shown in Fig. 2, was designed so that the leading $m = 1$ moment nominally occurred in $l = 7$ multipole order. The odd-l intrinsic moments of the test bodies vanish by symmetry, while the $l = 2$ and $l = 4$ moments vanish by design. However, construction imperfections produced stray pendulum moments in $l = 2$ and $l = 3$ orders. The Pb and Cu bodies had nominally identical external dimensions, masses, and surface properties. The Cu bodies were solid cylinders machined from 99.996% pure material. The Pb bodies were made from a 92% Pb/7.75% Sb/0.25% Sn alloy for good machinability, and contained cavities to account for their greater density. The test bodies were placed on a Be pendulum tray that held four mirrors for monitoring the pendulum twist and two passive compensator masses that made the q_{20} moment of the entire pendulum vanish. The test bodies were located in machined recesses, allowing us to interchange them and reverse the composition dipole without altering the rest of the instrument. These interchanges provided a powerful way to distinguish a UFF-violating effect from imperfections in the pendulum tray, suspension system, etc. The composition dipole along with the rest of the pendulum and suspension fiber could be reversed with respect to the remainder of the apparatus by rotating the fiber's upper attachment by 180°.

The entire pendulum was coated with Au and suspended inside a Au-coated magnetic shield by a 80 cm long, 20 μm diameter Au-coated W fiber with a torsional constant $\kappa = 0.0316$ erg/radian. The pendulum free-oscillation period was $\tau_0 = 747.4$ s; the amplitude

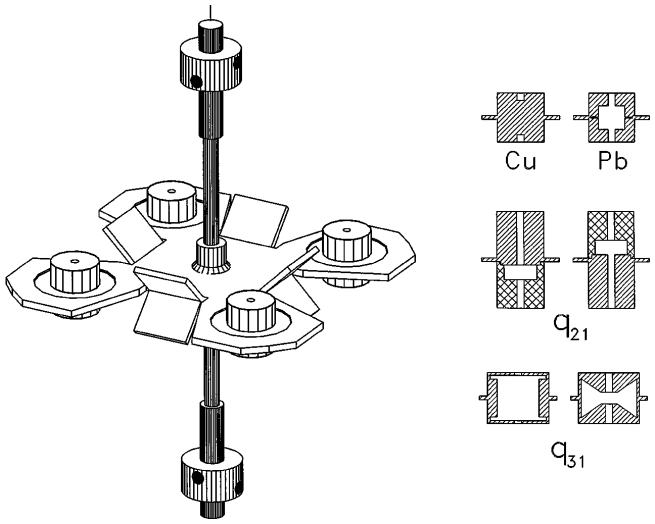

FIG. 2. The torsion pendulum. Small screws in the compensator masses on the ends of the vertical shaft were adjusted to reduce the stray q_{21} and q_{31} moments of the pendulum. The test bodies, shown in cross section in the inset, have masses that are identical to within 0.39 mg. The inset also shows the bodies used to turn the pendulum into q_{21} or q_{31} gradiometers with vanishing composition dipole moments.

damping time was 5×10^5 s at our operating vacuum of 1×10^{-6} Torr. The pendulum twist was monitored by an autocollimator that reflected light off one of the mirrors on the pendulum.

A computer monitored the pendulum twist, the attractor orientation, the tilts of the torsion balance and of the attractor turntable, and the temperatures at 12 or more locations. Horizontal and vertical seismic accelerations were also monitored in some of the data. The attractor revolution period and data recording interval were $\tau_A = 1.5\tau_0$ and $\tau_R = \tau_A/48$, respectively. Data were accumulated continuously, and cut into segments containing exactly 6 attractor revolutions. Data from each "cut" were analyzed by applying a digital filter that eliminated the free torsional oscillations and fitting the filtered twist, θ, as a function of ϕ

$$\theta(\phi) = \sum_{n=1}^{5} a_n \sin n\phi + b_n \cos n\phi + \sum_{m=1}^{3} d_m P_m(x), \tag{5}$$

where P_m is a Legendre polynomial whose argument x is proportional to time. The polynomials accounted for a continuous unwinding of the torsion fiber that, after heat treating, was ≤ 1 μrad/h. The harmonic sum ran up to $n = 5$ because a 5ω torque was produced whenever the 4-fold symmetric pendulum was horizontally misaligned with respect to the revolution axis of the attractor. In fact, we used this 5ω signal to align the pendulum to within ± 0.04 mm of its proper horizontal position. The pendulum was positioned to within ± 0.06 mm of the vertical center of the attractor by installing q_{21} gradiometer bodies on the pendulum and putting the attractor in the Q_{31} position (see below), and then adjusting the pendulum height until the induced 1ω signal vanished.

Roughly equal amounts of data were taken on two opposite pendulum mirrors and for two opposite orientations of the composition dipole on the pendulum tray. The harmonic coefficients from Eq. (5) were corrected for pendulum inertia, electronic time constants, the filter, and systematic effects from gravity gradients. The corrected coefficients, $\tilde{a}_n$ and $\tilde{b}_n$ from $N = 257$ pairs of "cuts" with opposite orientations, $\mathcal{A}$ and $\mathcal{B}$, of the composition dipole on the tray, were fitted to generate our UFF-violating signal, S, and a quadrature null, Q,

$$S = \sum_{i=1}^{N} [(\tilde{a}_1)_i^{\mathcal{A}} + (\tilde{a}_1)_i^{\mathcal{B}}]/2N = -0.09 \pm 0.73 \text{ nrad}, \tag{6}$$

$$Q = \sum_{i=1}^{N} [(\tilde{b}_1)_i^{\mathcal{A}} + (\tilde{b}_1)_i^{\mathcal{B}}]/2N = +0.65 \pm 0.73 \text{ nrad}. \tag{7}$$

The S and Q values are consistent with zero (see Fig. 3) and lead to a 1σ result

$$a_{\text{Cu}} - a_{\text{Pb}} = (-0.7 \pm 5.4 \pm 1.9) \times 10^{-13} \text{ cm/s}^2; \tag{8}$$

the first error is statistical and the second systematic.

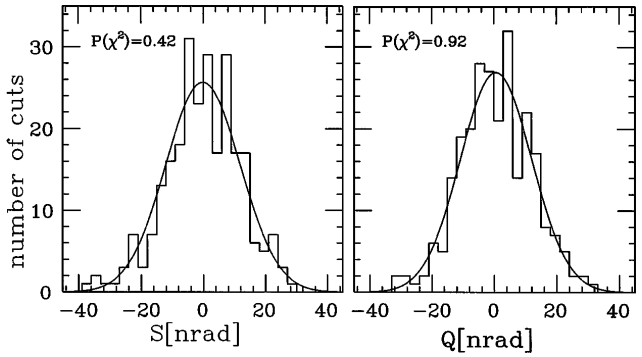

FIG. 3. Signal, S, and quadrature, Q, values for 257 pairs of data points with opposite orientations of the composition dipole on the pendulum tray. The curves are Gaussian fits to the histograms; the χ^2 probabilities are good in both cases.

Systematic effects were studied by identifying possible "driving terms" (gravity gradients, magnetism, temperature variations, and gradients, etc.) and making separate measurements in which, one at a time, each of these "driving terms" was deliberately introduced at a large enough level to cause a perceptible twist. The ratio of induced twist to driving term magnitude was our "sensitivity" to that driving term. These "sensitivities" were then multiplied by the measured value of the driving terms under normal operating conditions. Gravitation was the only systematic effect that warranted a correction. The uncertainty in the gravitational correction and the upper limits on other systematic effects (see Table I) were summed in quadrature to obtain our systematic error.

Two separate gravitational effects were involved: the 100 nrad gravitational "sidepull"deflection of the pendulum toward the attractor, and direct gravity-gradient torques given by Eq. (4). Sidepull twisted the pendulum by ≈ 6.5 nrad (via a mechanism related to the familiar "tilt effect") but canceled when we combined data from configurations $\mathcal{A}$ and $\mathcal{B}$ in our signal. Gravity-gradient torques were determined from Eq. (4) using measured stray q_{21} and q_{31} moments of the normal pendulum and stray Q_{21} and Q_{31} fields of the normal attractor. The stray moments were measured after every test-body interchange by rotating the attractor segments, as shown in Fig. 4, to produce large, well-known Q_{21} and Q_{31} fields. The stray Q_{21} and Q_{31} fields of the normal attractor were

TABLE I. 1σ systematic error budget.

Driving term	Normal magnitude	ΔS (nrad)
Gravity-gradient correction	5.8 nrad	± 0.17
$L = 4$ gravity gradients		± 0.18
1ω temperature fluctuations	0.04 ± 0.01 mK	± 0.05
1ω temperature gradients	1.02 ± 0.04 mK	± 0.01
1ω magnetic fields	0.2 mG	± 0.01
1ω tilt	0.42 ± 0.42 nrad	± 0.03

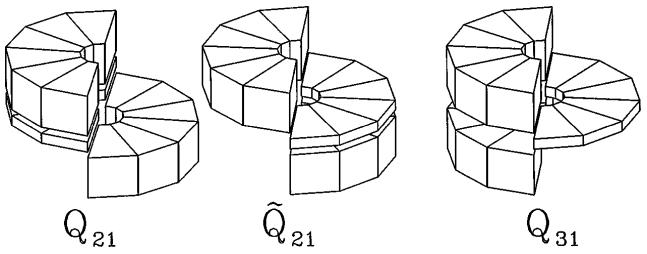

FIG. 4. Attractor configurations used to measure stray pendulum moments. The q_{21} moment was measured by averaging data taken with the Q_{21} and $\tilde{Q}_{21}$ attractor configurations; the q_{31} moment was found using the Q_{31} configuration.

always measured after it was returned to its normal configuration by loading the pendulum with special gradiometer test bodies, shown in Fig. 2, that gave the pendulum large and well-known q_{21} or q_{31} moments. The net gravity-gradient corrections to S and Q were 5.8 and 0.5 nrad, respectively. We tested the accuracy of our gravity-gradient correction procedure by operating a pendulum with deliberately exaggerated q_{21} and q_{31} moments in the field ofan attractor with large Q_{21} and Q_{31} gradients. The calculated gravity-gradient torque agreed to better than 3% with the observed twist. Direct measurements of the Q_{41} field and indirect measurements of the q_{41} moments indicate that $L = 4$ gravity gradients contributed an error of 0.18 nrad.

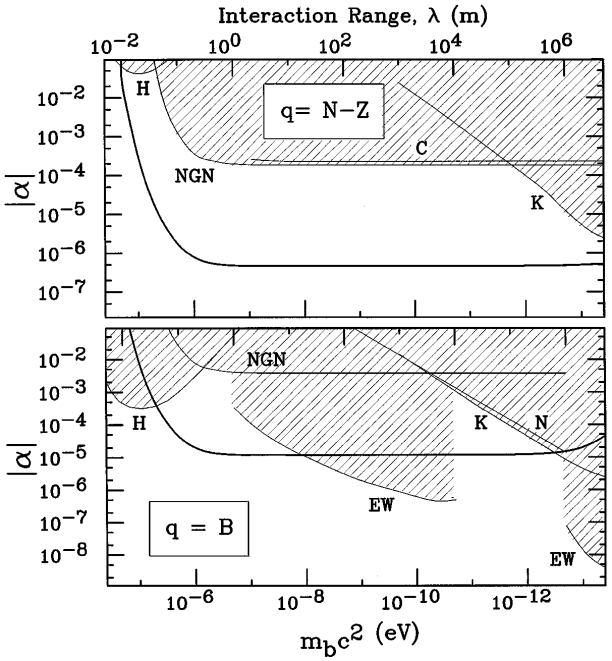

FIG. 5. 2σ constraints on $|\alpha|$ vs λ. The heavy curves are from this work; the shaded region shows previous results. We improved the $q = B = N + Z$ constraints by factors of 300 at $\lambda \approx 0.5$ m and up to 100 in the gap region; the $q = N - Z$ constraints are better by a factor of 300. Previous results are labeled: EW Ref. [3, NGN Ref. [9], N Ref. [6], K Ref. [7], C Ref. [10], B Ref. [11], and H Ref. [13].

TABLE II. 1σ limits on the strength, Λ_N, of power-law potentials.

N	This work	Ref. [12]
1	6×10^{-48} [a]	1×10^{-47}
2	4×10^{-30}	1×10^{-26}
3	6×10^{-16}	1×10^{-12}

[a]Using Ref. [3].

We now use the result in Eq. (8) to constrain possible equivalence-principle violating interactions. Figure 5 shows limits on α_5 as a function of λ for two possible choices for the "charge," $q = N - Z$ and $q = B$, where $B = N + Z$ is the baryon number [8]. Constraints for other possible charges can be obtained by scaling the results shown in Fig. 5. We have substantially strengthened previous constraints [9,10] on interactions with $q = N - Z$ and rule out an earlier suggestion [11] of such an interaction. Our results set improved constraints on interactions with $q = B$ in the regimes $0.05 \leq \lambda \leq 80$ m and $10^4 \leq \lambda \leq 10^6$ m.

The results in Fig. 5 and Eq. (8) also constrain power-law potentials, discussed by Feinberg and Sucher [12] in the context of multigluon exchange. Table II compares our limits on such potentials, $V(r) = \Lambda_N (r_0/r)^{N-1} \hbar c/r$ where $r_0 = 1$ fm, to those obtained in Ref. [12].

This work was supported by NSF Grants No. PHY-9104541 and No. PHY-9602494. We thank the DOE for the high-purity depleted uranium. Undergraduates Tim Bast, Kim Mauldin, Chris Polly, Hans Vija, and Jörn Häuser contributed to the apparatus development.

[1] P. G. Roll, R. Krotkov, and R. H. Dicke, Ann. Phys. (N.Y.) **26**, 442 (1964).
[2] V. B. Braginsky and V. I. Panov, Zh. Eksp. Teor. Fiz. **61**, 873 (1971) [Sov. Phys. JETP **34**, 463 (1972)].
[3] Y. Su *et al.*, Phys. Rev. D **50**, 3614 (1994).
[4] This is the average density of our uranium including the effects of voids and Zn coating.
[5] E. G. Adelberger *et al.*, Phys. Rev. D **42**, 3267 (1990).
[6] T. M. Niebauer, M. P. McHugh, and J. E. Faller, Phys. Rev. Lett. **59**, 609 (1987).
[7] K. Kuroda and M. Mio, Phys. Rev. D **42**, 3903 (1990).
[8] Our $q = B$ constraints weaken for $\lambda \geq R_\oplus$, where $R_\oplus$ is the Earth radius. Because the attractor and Earth have very similar (B/μ) values, the Yukawa and gravitational forces become proportional when $\lambda \gg R_\oplus$. The attractor's modulation of local vertical then causes the Yukawa interactions of the test bodies with Earth to almost cancel their Yukawa interactions with the attractor.
[9] P. G. Nelson *et al.*, Phys. Rev. D **42**, 963 (1990).
[10] R. Cowsik *et al.*, Phys. Rev. Lett. **64**, 336 (1990).
[11] P. E. Boynton *et al.*, Phys. Rev. Lett. **59**, 1385 (1987).
[12] G. Feinberg and J. Sucher, Phys. Rev. D **20**, 1717 (1979).
[13] J. K. Hoskins *et al.*, Phys. Rev. D **32**, 3084 (1985).